Fig. S1

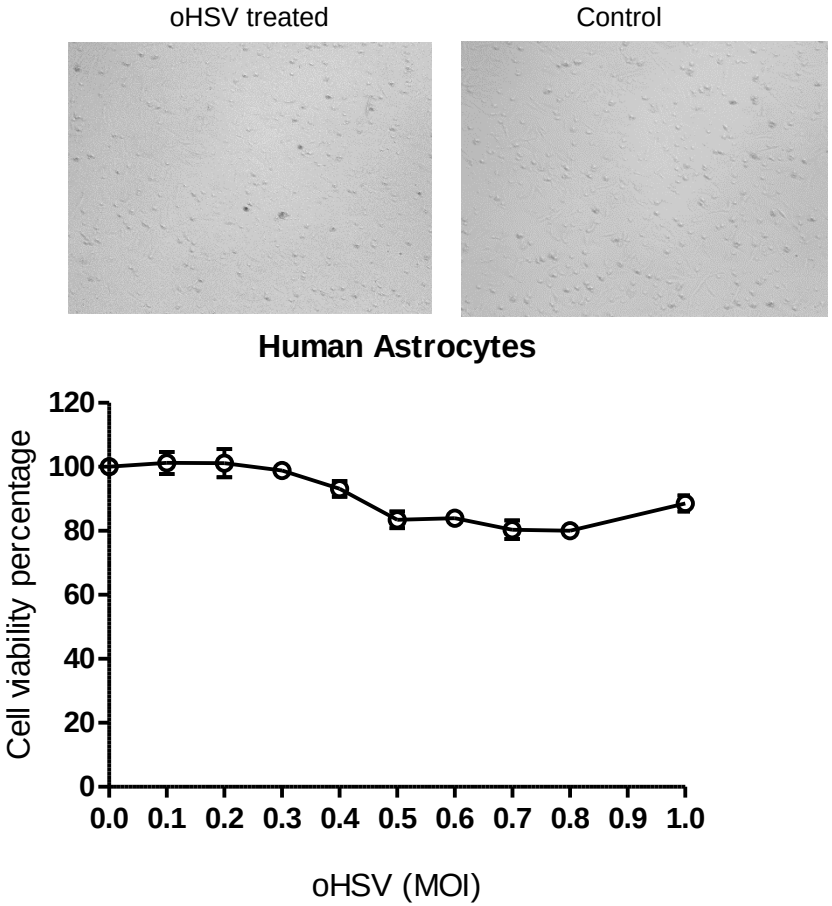
oHSV treated
Control
Human Astrocytes
Cell viability percentage
120
100
80
60
40
20
0
0.0 0.1 0.2 0.3 0.4 0.5 0.6 0.7 0.8 0.9 1.0
oHSV (MOI)

Fig. S2

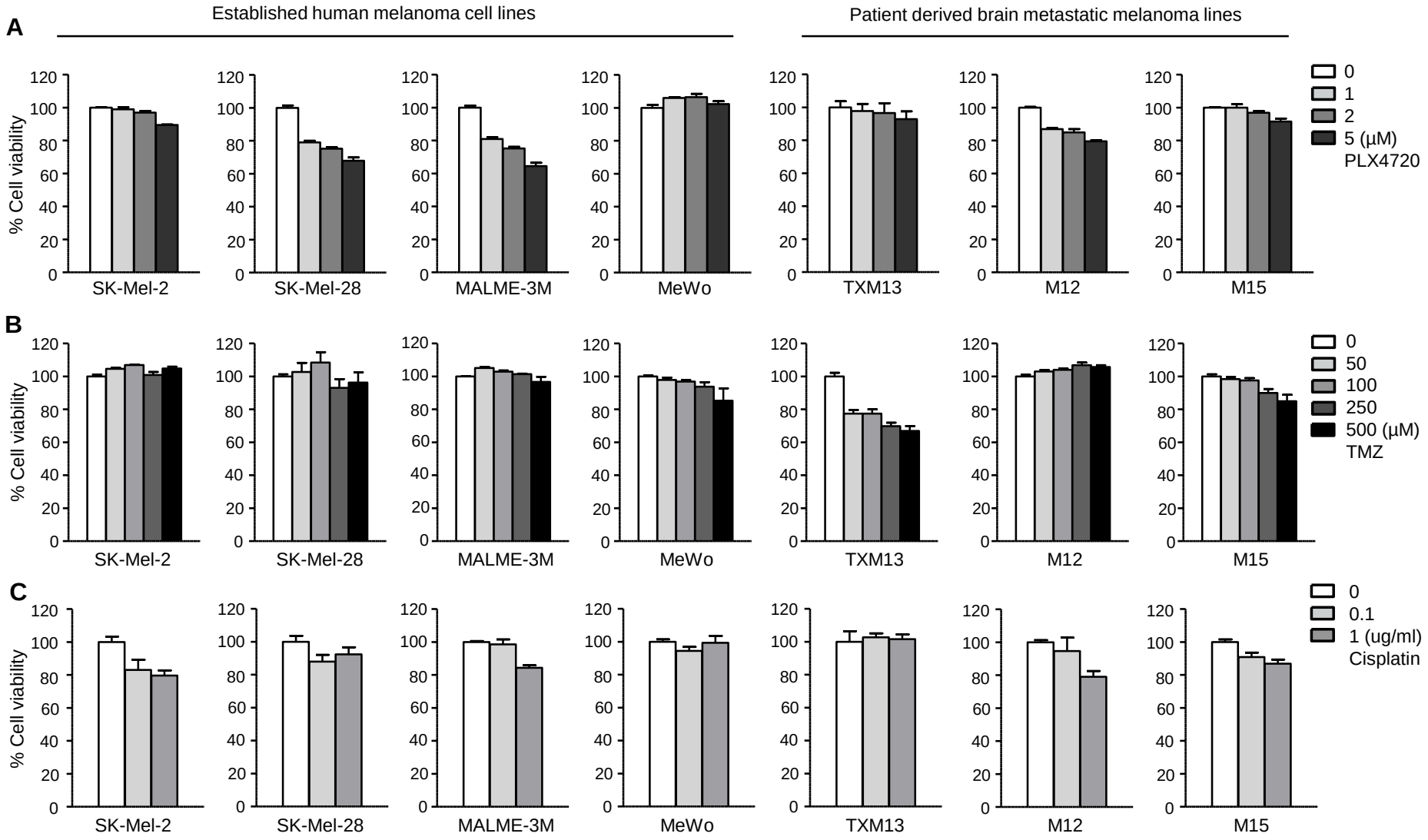
A
Established human melanoma cell lines
Patient derived brain metastatic melanoma lines
% Cell viability
SK-Mel-2
SK-Mel-28
MALME-3M
MeWo
TXM13
M12
M15
0
1
2
5 (µM)
PLX4720
B
0
50
100
250
500 (µM)
TMZ
C
0
0.1
1 (ug/ml)
Cisplatin

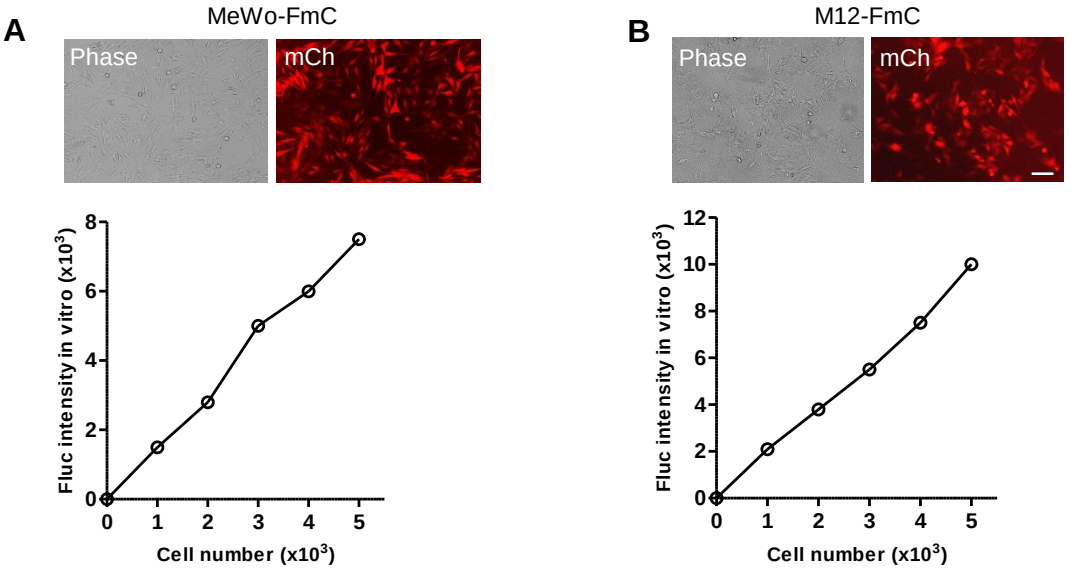
A
MeWo-FmC
Phase
mCh
Fluc intensity in vitro (x10^3)
Cell number (x10^3)
B
M12-FmC
Phase
mCh
Fluc intensity in vitro (x10^3)
Cell number (x10^3)

Fig. S4

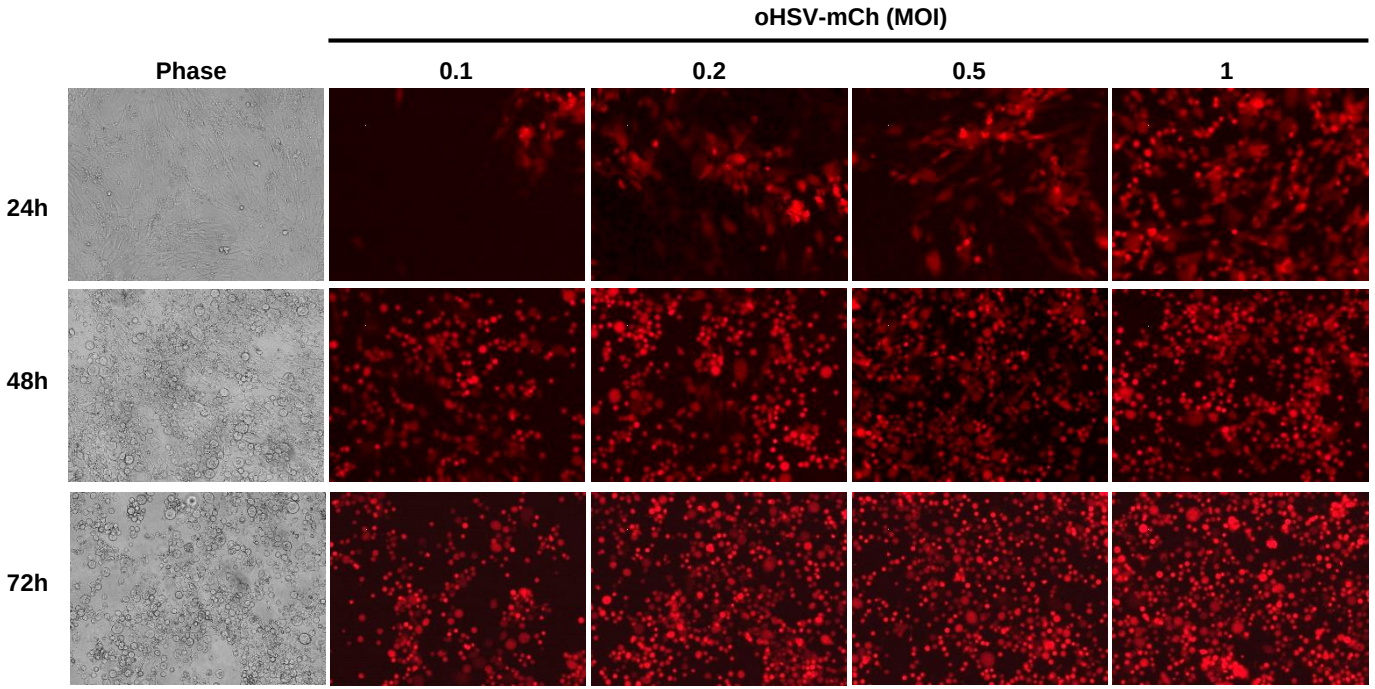

Fig. S5

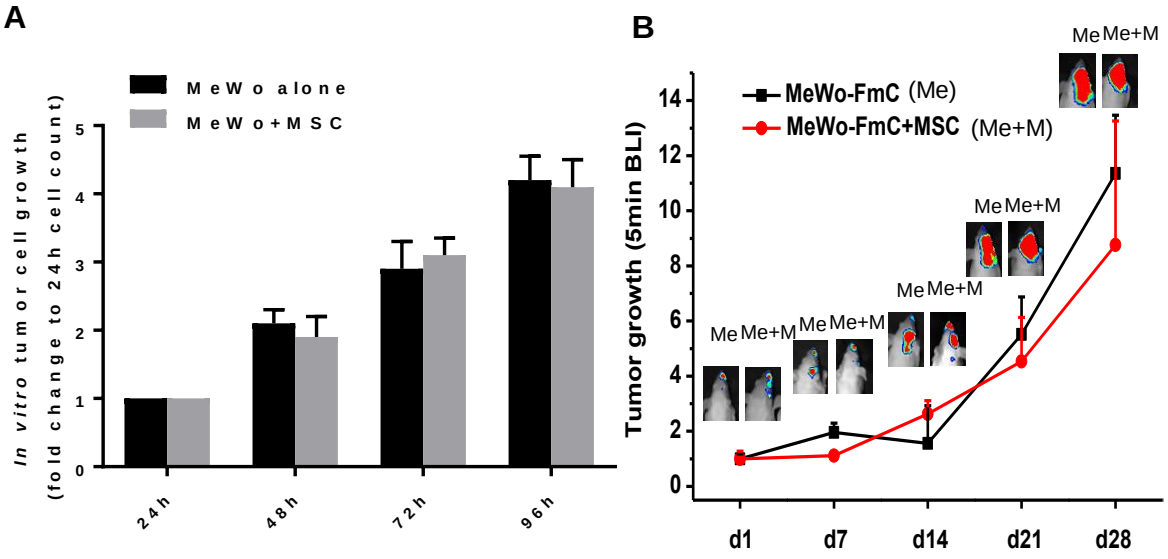
A
MeWo alone
MeWo+MSC
In vitro tumor cell growth
(fold change to 24h cell count)
0
1
2
3
4
5
24h
48h
72h
96h
B
MeWo-FmC (Me)
MeWo-FmC+MSC (Me+M)
Tumor growth (5min BLI)
0
2
4
6
8
10
12
14
d1
d7
d14
d21
d28
Me
Me+M

Fig. S6

A

Day 5, ICA injected MSC-oHSV-Fluc in brain tumor bearing mice

Fluc Imaging

B

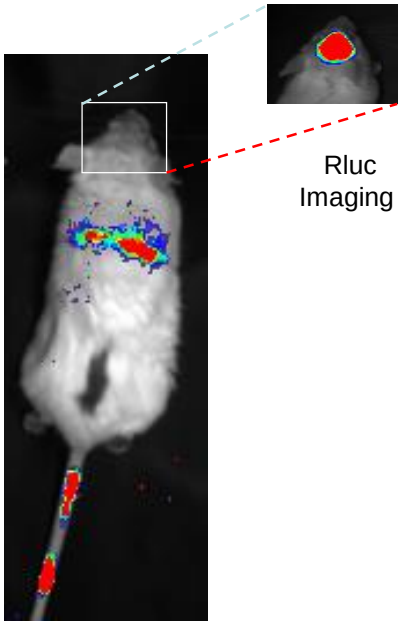

Rluc Imaging

Fluc Imaging

Fig. S7

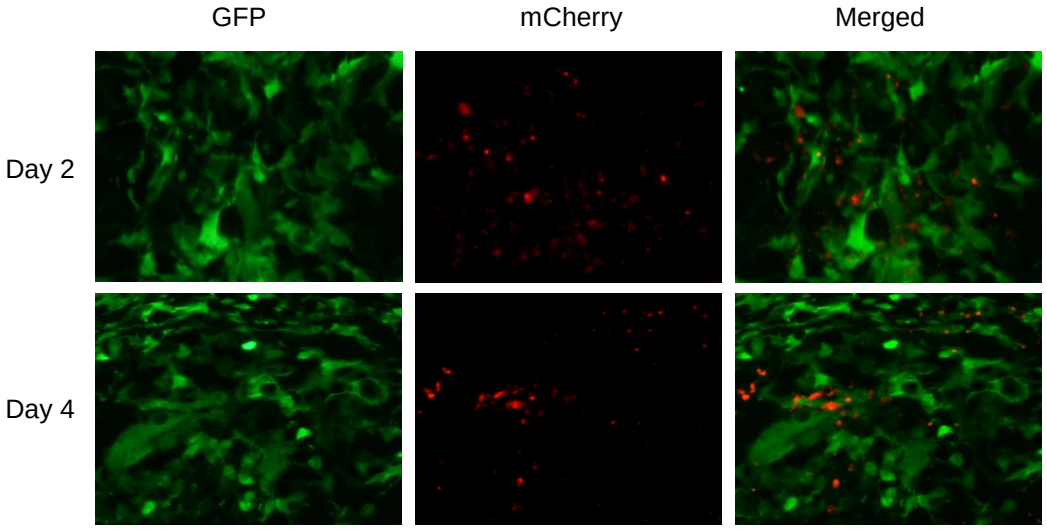

Fig. S8

A

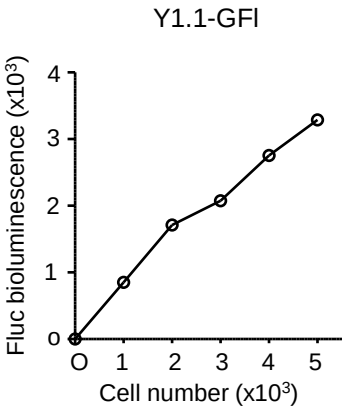

B

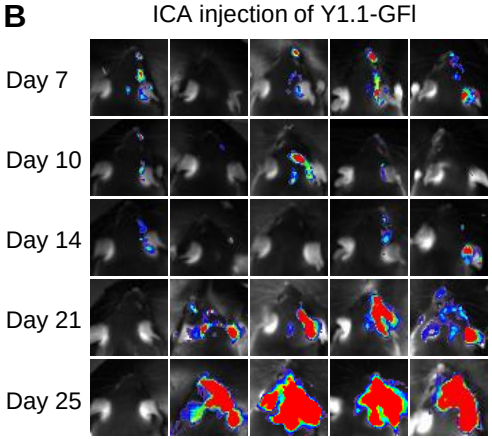

C

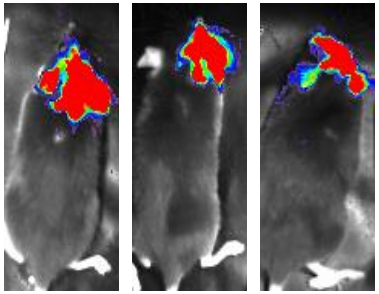

Day 25 after ICA injection of Y1.1-GFl
Whole BLI images

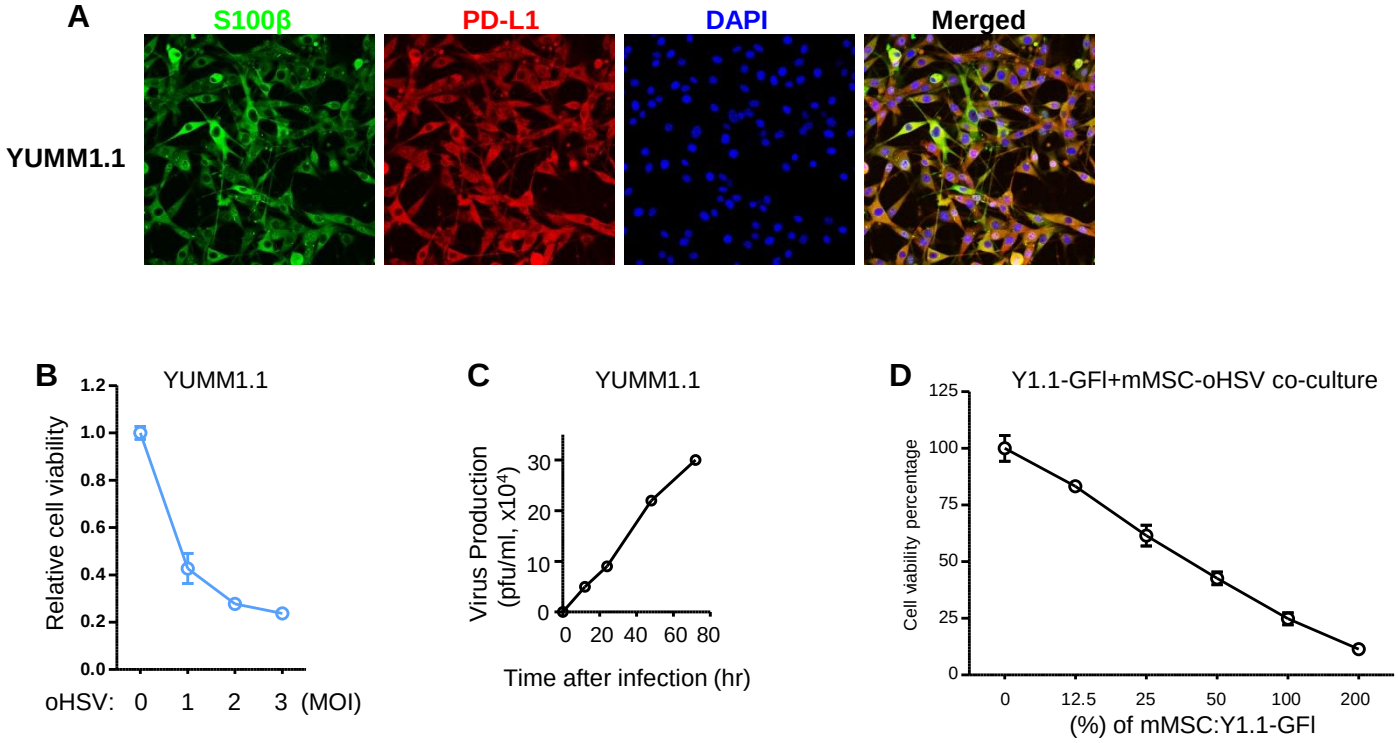
A
S100β
PD-L1
DAPI
Merged
YUMM1.1
B
YUMM1.1
Relative cell viability
1.2
1.0
0.8
0.6
0.4
0.2
0.0
oHSV: 0 1 2 3 (MOI)
C
YUMM1.1
Virus Production (pfu/ml, x10⁴)
30
20
10
0
0 20 40 60 80
Time after infection (hr)
D
Y1.1-GFl+mMSC-oHSV co-culture
Cell viability percentage
125
100
75
50
25
0
0 12.5 25 50 100 200
(%) of mMSC:Y1.1-GFl

Fig. S10

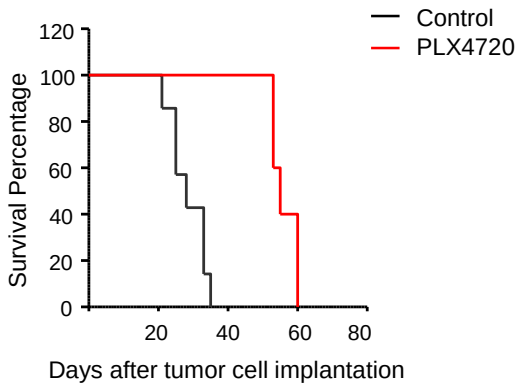
Control
PLX4720
120
100
80
60
40
20
0
Survival Percentage
20
40
60
80
Days after tumor cell implantation

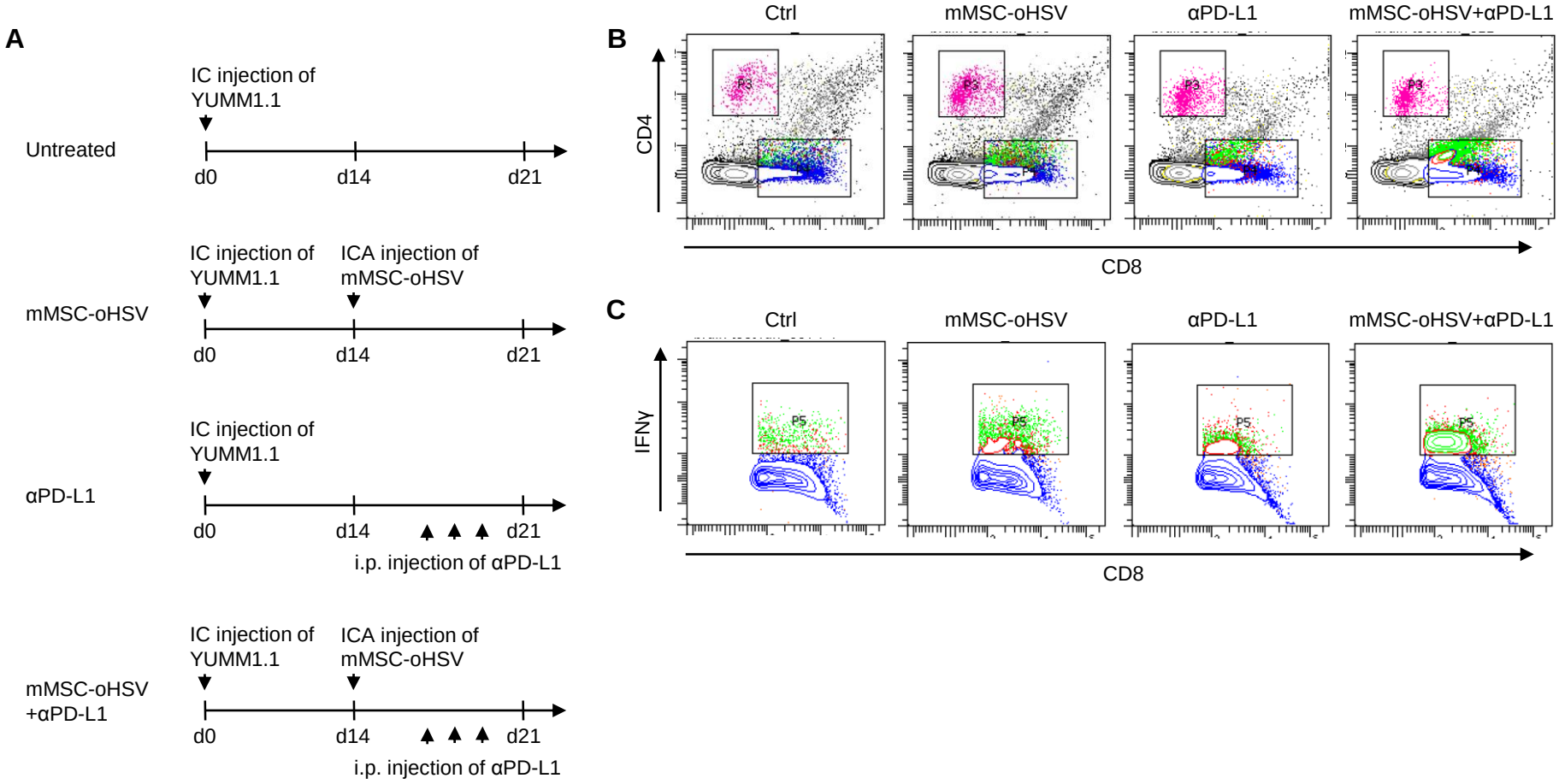
A
IC injection of YUMM1.1
Untreated
d0
d14
d21
IC injection of YUMM1.1
ICA injection of mMSC-oHSV
mMSC-oHSV
d0
d14
d21
IC injection of YUMM1.1
αPD-L1
d0
d14
d21
i.p. injection of αPD-L1
IC injection of YUMM1.1
ICA injection of mMSC-oHSV
mMSC-oHSV +αPD-L1
d0
d14
d21
i.p. injection of αPD-L1
B
Ctrl
mMSC-oHSV
αPD-L1
mMSC-oHSV+αPD-L1
CD4
CD8
C
Ctrl
mMSC-oHSV
αPD-L1
mMSC-oHSV+αPD-L1
IFNγ
CD8

Fig. S12

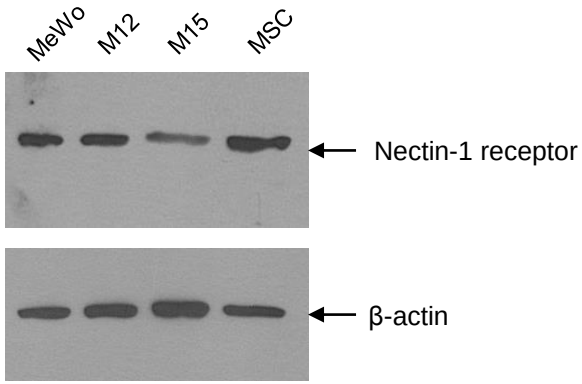

Fig. S13

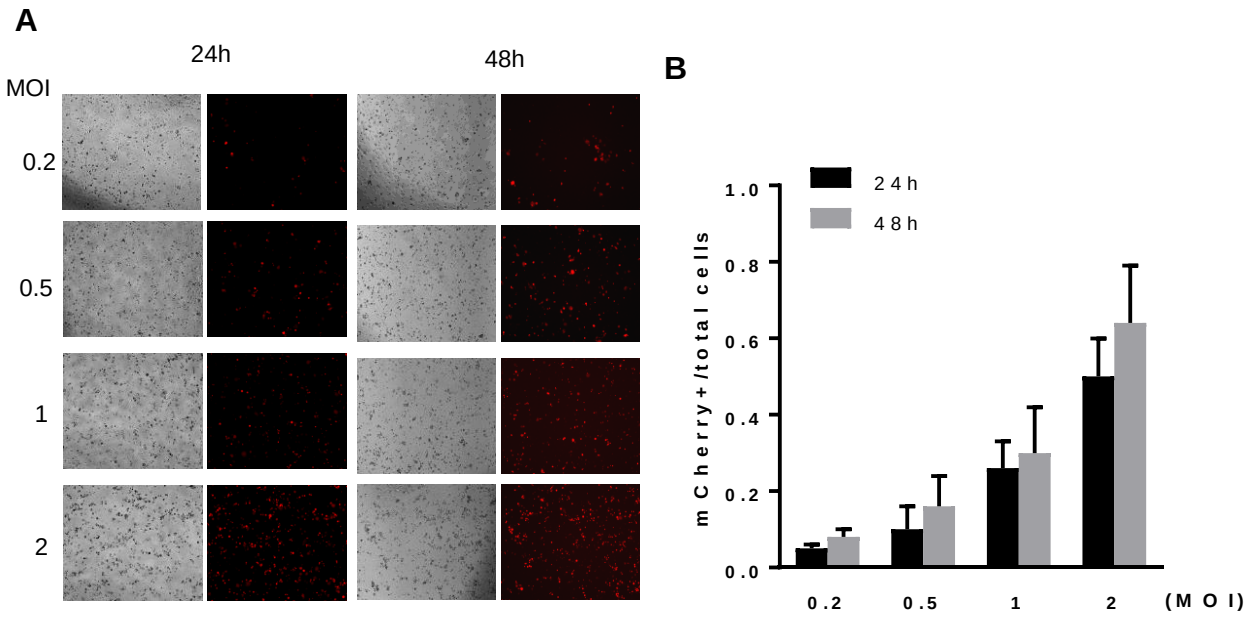
A
24h
48h
MOI
0.2
0.5
1
2
B
24h
48h
mCherry+/total cells
1.0
0.8
0.6
0.4
0.2
0.0
0.2
0.5
1
2
(MOI)

Fig. S14

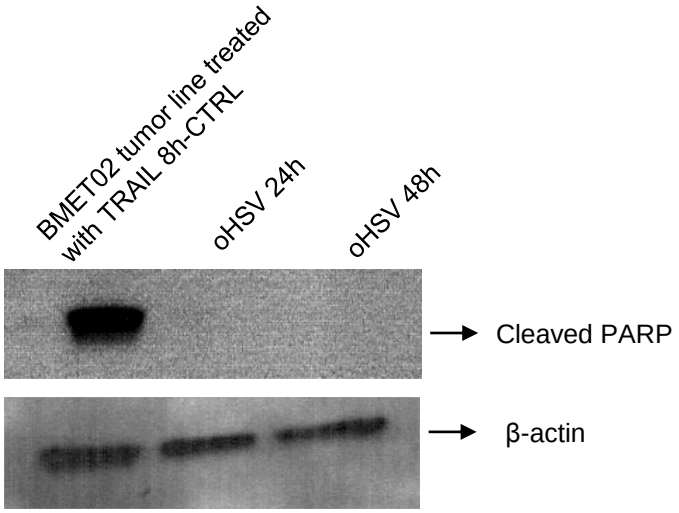
BMET02 tumor line treated with TRAIL 8h-CTRL
oHSV 24h
oHSV 48h
Cleaved PARP
β-actin

Supplementary Figure legends

Supplementary Figure 1. Plot and representative images showing the cell viability of human astrocytes infected with oHSV at different MOI 4 days post infection.

Supplementary Figure 2. Responses of multiple human melanoma lines to PLX4720, TMZ and Cisplatin. Plots showing cell viabilities of melanoma lines treated with PLX4720 (A), TMZ (B) and low dose Cisplatin (C) at indicated concentrations.

Supplementary Figure 3. Characterization of engineered MeWo-FmC and M12-FmC. (A, B) Upper, representative phase and fluorescent images of engineered MeWo-FmC and M12-FmC lines. Lower, correlation between cell number and *in vitro* Fluc bioluminescence signal was analyzed.

Supplementary Figure 4. Representative phase and fluorescent images of human MSC transduced with oHSV-mCh at different MOI over time.

Supplementary Figure 5. (A) Plot showing MeWo-GFP tumor cell growth over time in the presence and absence of MSC in co-culture settings. (B) *In vivo* bioluminescence imaging of MeWo-FmC tumor growth over time in mice brains with or without ICA injection of MSC.

Supplementary Figure 6: (A) Fluc bioluminescent images of brain tumor bearing mice treated with ICA injection of MSC-oHSV-Fluc. (B) Human MSC expressing firefly luciferase (Fluc) were incubated with oHSV for 6 hours and injected via tail vein in mice bearing MeWo-Rluc tumors. Fluc bioluminescent image showing the fate of MSC 24 hrs post-injection. (Inset) Rluc bioluminescent image showing MeWo-Rluc tumor in the brain.

Supplementary Figure 7. Fluorescent images from brain sections of mice showing the population of M12-GFP-Fluc tumor cells (GFP^+) and MSC-oHSV-mCh cells (mCh^+) at indicated time points post-ICA injection of MSC-oHSV-mCh in M12-GFP-Fluc tumor bearing mice.

Supplementary Figure 8. Characterization of engineered Y1.1-GFl. (A) Linear correlation between Y1.1 engineered to express GFP-firefly luciferase (Y1.1-GFl) cell number and *in vitro* Fluc bioluminescence

signal. (B) Representative bioluminescent images of mice ICA injected with Y1.1-GFl at various time points post tumor cells implantation. (C) Whole body BLI images of mice with ICA injected Y1.1-GFl.

Supplementary Figure 9. Characterization of YUMM1.1 *in vitro*. (A) Immunocytochemistry analysis of S100β and PD-L1 staining in YUMM1.1 cells. (B) Cell viability of YUMM1.1 cells infected with oHSV at indicated MOI. (C) Plots showing oHSV virus production within YUMM1.1 cells infected with oHSV at MOI=0.5 over time. (D) Plot showing cell viability of Y1.1-GFl cells in co-cultures of Y1.1-GFl and mMSC-oHSV at indicated portions.

Supplementary Figure 10. Kaplan-Meier survival curves of melanoma brain metastasis bearing mice treated with PLX4720 (low dose chow food, n=5 mice) or untreated (n=7 mice). p=0.0011 in PLX4720 and control comparison, log-rank test.

Supplementary Figure 11. Flow cytometry analysis of tumor infiltrating lymphocytes in syngeneic mouse model. (A) Experiment outline. (B, C) Representative density plots for CD4, CD8 and IFNγ staining from the four groups of mice, tumor only (untreated control group), tumor+mMSC-oHSV, tumor+αPD-L1 and tumor+mMSC-oHSV+αPD-L1 treated groups.

Supplementary Figure 12. Western blot analysis showing nectin-1 receptor expression levels in MeWo, M12, M15 melanoma lines and human MSC.

Supplementary Figure 13. (A) Representative images of M15 infected with oHSV at indicated MOIs over time. (B) Plot showing the percentage of oHSV infected M15 cell populations at indicated time points.

Supplementary Figure 14. Western blot analysis showing cleaved PARP levels in both MeWo cells treated with oHSV after 24 and 48 hrs and in breast cancer cell line, BMET02 tumor line treated with TRAIL for 8 hrs as a positive control for cleaved PARP.

Supplementary Methods

Cell viability assays and oHSV production assay: The effect of oHSV on tumor cell viability and astrocytes was measured using CellTiterGlo (Promega, Madison, WI, USA) 4 days post virus infection with different MOI. All experiments were performed in triplicates. For the viral production assay, tumor cells plated on 12-well plates were infected with oHSV at MOI=0.2. After oHSV adsorption, media was replaced and culture continued. Twelve, 24, 48 and 72 hours post oHSV infection, culture supernatants were harvested. Titers of infectious oHSV were determined by plaque assay on Vero cells (American Type Culture Collection, Manassas, MA).

Co-cultures of MSC and melanoma cells: MSC or mMSC were freshly infected with oHSV-mCh (MOI=2) for 2 hrs, washed with PBS 3 times and then co-cultured with MeWo-GFP or Y1.1-GFl cells at indicated ratio on 24-well plate ($0.5x10^5$/well; Costar) in MSC culture medium. MeWo cells were then assessed for both the infection of oHSV-mCh and the cell lysis caused by oHSV infection via counting the GFP^+ and $mCherry^+$ cell numbers. Cell viability assay of Y1.1-GFl cells was performed by measuring the *in vitro* Fluc bioluminescence as previously described (1). In parallel, MeWo-GFP-Fluc cells were cultured alone or co-cultured with MSC at 1:1 ratio in a 24-well plate ($0.5x10^5$/well; Costar) in MSC culture medium. Cell viability assay of MeWo cells was performed by measuring the *in vitro* Fluc bioluminescence as described above.

Melanoma brain metastasis mouse models: Mice (6~8 weeks of age, Charles River Laboratories, Wilmington, MA) were anesthetized with ketamine-xylazine and an incision was made to expose the right carotid artery. Using 8-0 sutures, both common and internal carotid arteries were temporally ligated and a catheter connected to a 1ml syringe was inserted into the external carotid artery to inject tumor cells. Two hundred thousand MeWo-FmC or M12-FmC melanoma tumor cells suspended in 100 µl PBS were slowly injected through the catheter. The external artery was then permanently ligated under the dissecting scope (Olympus, SZX10) using fine surgical tools and blood circulation was restored by releasing both common and internal carotid blood flow. Mice were imaged for the success of tumor cell injection 7 days post-implantation and then periodically for tumor progression by *in vivo* BLI. In addition,

the number of metastatic lesions was defined by measuring the number of mCherry-positive foci using ImageJ tools (NIH). Accordingly, each composite image was subjected to ImageJ particle analysis and the number of mCherry-positive particles per section was plotted. Similar procedures were performed to develop syngeneic mouse tumor model using $2x10^5$ Y1.1-GFl in C57BL6 mice. Mice were imaged for tumor cell presence 7 days post-implantation and then periodically for tumor progression by *in vivo* BLI. All *in vivo* procedures were approved by the Subcommittee on Research Animal Care at Massachusetts General Hospital.

Western blot analysis of nectin-1 and cleaved PARP: MeWo, M12, M15 and human MSC cultures were collected and protein lysates were prepared by standard method. Commercial 4~12% Tris-Glycine SDS-Gel were used for all western blots. BMET02 cells were treated with TRAIL for 8 hrs, while MeWo cells were treated with oHSV for 24 or 48 hrs, cell lysates were collected for western blot assay. Nectin-1 antibody was purchased from R&D, cl-PARP and β-actin antibodies are from Cell Signaling.

***In vivo* studies with human melanoma lines:** Female SCID mice (6-8 weeks old) obtained from Charles River laboratories (Wilmington, MA) were used in four different *in vivo* experiments. 1) To track the fate of oHSV delivered by MSC and the dynamics of oHSV spread *in vivo*, MSC were infected with oHSV-Fluc (MOI=2) for 2 hrs, washed with PBS 3 times and 200,000 MSC-oHSV-Fluc cells were intracarotidly injected into either naive mice (without brain tumor, n=3) or brain tumor bearing mice (100,000 MeWo-GFP cells were intracranial implanted into the mice brains 14 days prior to MSC-oHSV-Fluc injection, n=3). The fate of oHSV was assessed by Fluc bioluminescence imaging over time as described previously (2). 2) To directly visualize the distribution of oHSV delivered by MSC in tumor bearing mice, 200,000 MSC cells loaded with oHSV-mCherry (MOI=2) were ICA injected into mice bearing MeWo-GFP or M12-GFP-Fluc brain tumors as described above. oHSV distribution was assessed by fluorescence microscopy on brain sections obtained post MSC-oHSV-mCh injection (48h, 72h and 120h, n=3 mice per time points, 3-5 brain sections from each mice were analyzed). Briefly, mice were sacrificed and brains were dissected as described previously. Fourteen μM sections were assessed for GFP and mCherry representing tumor cells and oHSV, respectively. Higher magnification images

were acquired with Olympus Digital Imaging Software (CellSens). Detailed section analysis was performed using Confocal microscopy (LSM Pascal, Zeiss). 3) To test the therapeutic potential of MSC-oHSV in melanoma brain metastasis, $2x10^5$ MeWo-FmC or M12-FmC cells were ICA injected into SCID mice (surgical manipulation was performed on ECA, and CCA was still intact at this time) and the metastatic tumor growth in the brain was further confirmed by *in vivo* BLI. Two weeks post-tumor cell injection, mice bearing metastatic brain tumors were treated with either MSC or MSC-oHSV via ipsilateral ICA administration and CCA was then permanently closed or ipsilateral ICA injection for the first treatment plus contralateral ICA injection for the second treatment. Mice were then followed for changes in brain tumor volumes by BLI as well as survival analysis. 4) To study the influence of naïve MSC on MeWo tumor growth, mice bearing MeWo-FmC tumors (n=10) were ICA injected with MSC (200,000 cells per mouse, n=5) or PBS (n=5). Mice were then followed for changes in brain tumor volumes by BLI.

***In vivo* studies with mouse melanoma lines:** To test the therapeutic potential of mMSC-oHSV in melanoma brain metastasis, $2x10^5$ Y1.1-GFl were ICA injected into C57BL6 mice and the metastatic tumor growth in the brain was followed by *in vivo* BLI. Two weeks post-tumor cell injection, mice bearing metastatic brain tumors were divided into four groups, untreated control group, mMSC-oHSV treated group (200,000 mMSC-oHSV were ICA injected on d14), anti-PD-L1 treated group (200, 100 and 100 µg anti-PD-L1 antibody (10F9G2) were intraperitoneally (i.p.) injected on d17, d18 and d20 respectively), and mMSC-oHSV plus anti-PD-L1 treated group (mMSC-oHSV were ICA administrated at d14, followed by i.p. injection of anti-PD-L1 at d17, d18 and d20 respectively). Mice were then followed for survival analysis and immunohistochemistry.

Flow cytometric analysis of tumor-infiltrating lymphocytes: To analyze the tumor-infiltrating lymphocyte populations post treatment, C57BL/6 mice were intracranially implanted with YUMM1.1 metastatic brain tumors (d0), two weeks post tumor cells implantation, brain tumor bearing mice were divided into four groups, untreated control group; mMSC-oHSV treated group in which 200,000 mMSC-oHSV cells were ICA administrated in each mouse at d14; anti-PD-L1 treated group in which PD-L1 antibody (10F9G2) were i.p. injected in mice at d17 (200ug/100ul PBS per mouse), d18 (100ug) and d20

(100ug) respectively; and the combination treatment of mMSC-oHSV+anti-PD-L1 group in which mMSC-oHSV were ICA administrated at d14, followed by i.p. injection of anti-PD-L1 at d17, d18 and d20 respectively. At d21, all the mice were sacrificed and brain tumors were harvested, minced with grinder, and digested with DNase I and Collagenase D, followed by Percoll gradient centrifugation to obtain TIL. Next, the samples were resuspended in FACS buffer for staining of mouse CD4-PE and CD8-PE-Cy7 (eBioscience); and intracellular staining was performed for mouse IFNγ-FITC (eBioscience). Samples were run on a BD LSRII Flow Cytometer (BD Biosciences) and data were analyzed using FlowJo Software version 7.6.5 (Tree Star).

References:

1. Bagci-Onder T, Du W, Figueiredo JL, Martinez-Quintanilla J, & Shah K (2015) Targeting breast to brain metastatic tumours with death receptor ligand expressing therapeutic stem cells. *Brain : a journal of neurology* 138(Pt 6):1710-1721.
2. Tamura K*, et al.* (2013) Multimechanistic tumor targeted oncolytic virus overcomes resistance in brain tumors. *Molecular therapy : the journal of the American Society of Gene Therapy* 21(1):68-77.